Defence Science Journal, Vol. 61, No. 4, July 2011, pp. 370-376, DOI: 10.14429/dsj.61.89

Broadband Passive Sonar Signal Simulation in a Shallow Ocean

Baiju M. Nair*, K.P. Arunkumar, and Sudha B. Menon

Naval Physical and Oceanographic Laboratory, Kochi-21
**E-mail: baiju_nair1@yahoo.com*

ABSTRACT

The broadband plane-wave model is valid only in the far-field of a point source under free-field propagating conditions. However the acoustics in ocean is characterised by multi-modal acoustic propagation due to its top-bottom limited boundary conditions. The effect of multi-modal field is to alter the source spectrum while the effect of dispersion is to modify the pulse shape. Moreover, using a plane-wave beam former in a multi-modal field leads to bias in the bearing estimates. These effects are highly dependant on the environment parameters and have important ramification for target localisation and classification in an ocean waveguide. A more realistic simulator has been proposed which essentially models these effects and therefore serves to provide test signals for first-hand verification of signal processing algorithms to be developed for such scenarios. This model is to be understood as a better model than the naïve plane-wave model which is entirely oblivious of even the gross features such as wave propagation in an oceanic waveguide. The channel parameter so estimated from the present simulation can be convolved with the radiated noise spectra of the source to generate passive sonar signal.

Keywords: Sonar signal simulation, shallow ocean, normal mode model, plane-wave model

1. INTRODUCTION

The signal noise simulator in the existing sonar systems implements a broadband plane-wave model. This model is valid only in the far-field of a point source under free-field propagating conditions. However, the acoustics in ocean is characterised by multi-modal acoustic propagation due to its top-bottom limited boundary conditions. In acoustic waveguide such as shallow water channel, sound propagates in terms of eigen functions of the channel (normal modes). Each of the modes can be interpreted as a plane-wave arriving at the receiver at a certain vertical incident angle. The bearing of the source relative to the array axis would be different in the free-field and in the oceanic waveguide. In case of free-field propagation, the incident wave would be a plane-wave arriving at the true source bearing. In a waveguide, the array receives a signal, which is a sum of several modes each of which can be viewed as a plane-wave arriving at its own vertical incidence angles. Consequently, the conventional plane-wave delay-sum beam-former as well as the frequency-domain beam-former yields incorrect (biased) estimates of the target's bearing. This bias increases as the target moves away from the broadside towards the end-fire of a linear array[1,2]. Another effect of the waveguide is to alter the source signal spectrum due to varying gain and phase modification across the frequencies[3,4]. Also, conventional active sonar detection involves basebanding, match filtering, and normalising the received time series. The envelope obtained is compared against a threshold. Cell-average constant false alarm rate (CA-CFAR) normalisation for the threshold estimation, derived without consideration of multipath environment is often incorrect[5]. Tao[6], *et al.* discusses the problem of suppressing moving end-fire interference incident on a horizontal towed array in shallow water. Mitigation of end-fire interference is especially important in passive sonar application since often the first detection of the target with a towed array occurs towards forward end-fire despite better bearing resolution at the broadside. Masking of targets by end-fire interference frequently occurs when multipath spread in elevation angle appears as spread in slant azimuth on horizontal array. The target scattered signature is often significantly distorted by multipath propagation, with such dependent on the sensing parameters, such as target and receiver location, water depth, seabed geoacoustic parameters, etc. The wideband, free-field bistatic scattered fields from targets have to be coupled with a separate model applied to simulate the channel, to yield the overall target-in-channel signatures[7, 8].

A more realistic simulator has been proposed which essentially models these effects, and therefore serves to provide test signals for first-hand verification of signal processing algorithms to be developed for such scenarios. This model is to be understood as a better model than the naïve plane-wave model which is entirely oblivious of even the gross features such as wave propagation in an oceanic waveguide. The simulation methodology has been described for synthesising the continuous broadband acoustic signal (as in a passive sonar) received by an array of sensors. The broadband signal is synthesised by composing several narrowband components spaced uniformly over the band of interest.

Received 24 March 2010, revised 21 March 2011, published online 25 July 2011

2. NARROW BAND SIGNAL SIMULATION

The two scenarios of wave propagation for the narrow band signal component simulation are

- Free-field plane wave propagation
- Oceanic waveguide propagation based on the normal mode theory.

2.1 Plane-wave Propagation Model

It was assumed that the array consists of M sensors located at position vectors $\{\boldsymbol{p}_m = (x_m, y_m, z_m): 1 \le m \le M\}$ wrt an arbitrary Euclidean coordinate system in 3-D space (Fig. 1). There are J broadband sources located at $\{\boldsymbol{r}_j = (x_j, y_j, z_j): 1 \le j \le J\}$. A position vector $\boldsymbol{r} = (x, y, z)$ which is in Cartesian coordinates, can be expressed in spherical coordinates as follows:

$$\boldsymbol{r} = r\,(\cos\phi.\cos\varphi,\ \sin\phi.\cos\varphi,\ \sin\varphi)^T \qquad (1)$$

where ϕ is the azimuth angle measured wrt the positive X-axis on XY plane and φ is the elevation angle as shown in Fig. 2. The same vector in cylindrical coordinates can be expressed as

$$\boldsymbol{r} = (r_{xy}.\cos\phi,\ r_{xy}.\sin\phi,\ z)^T \qquad (2)$$

where r_{xy} is the cylindrical range given by

$$r_{xy} = \sqrt{(x^2 + y^2)} \qquad (3)$$

Consider the array of sensors[10] located far away from several point sources in a free field (Fig. 2). In this case, the wave propagation across the array can be described by a sum of several plane-waves each due to one-point source. At each temporal frequency Ω in the frequency band of the source signal, a plane-wave is associated with a wave-number vector $\boldsymbol{K} = (K_x, K_y, K_z)$. The magnitude of this vector is Ω/c, where c is the speed of sound propagation (in m/s). The direction of this vector indicates the direction of the source from which it originated.

Let the signal due to j^{th} source at the origin of the coordinate system be

$$s_j(t) = \check{s}_j(t).\exp(i\Omega t) \qquad (4)$$

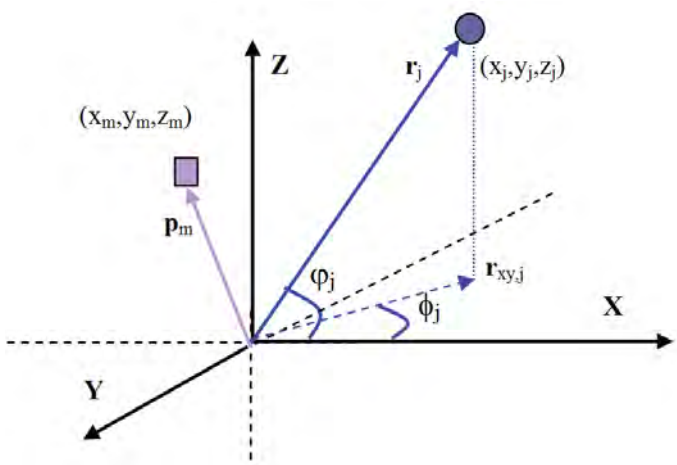

Figure 1. Coordinate system showing J^{th} source and m^{th} sensor in 3-D space.

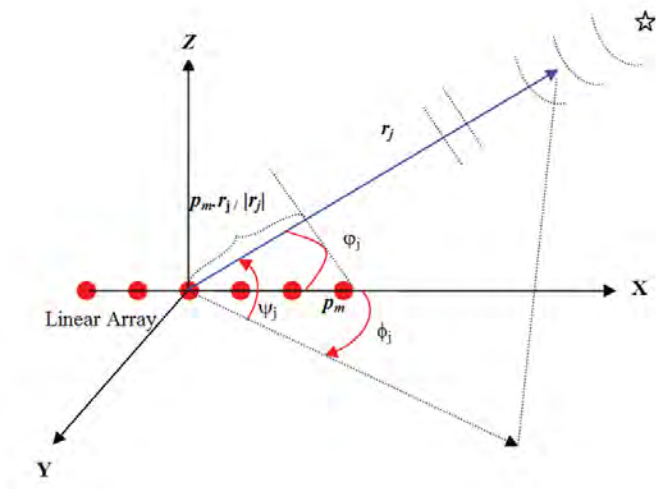

Figure 2. Plane-wave arrival.

where $\check{s}_j(t)$ is the slowly varying envelope of the narrowband signal $s_j(t)$ emitted from the source. The signal $\check{s}_j(t)$ is modelled as a low-pass random signal of small bandwidth $\Delta\Omega$ such that the variation of $\check{s}_j(t)$ can be neglected during the time taken by the plane-wave to pass the array. This is usually known as the narrow band assumption in array processing and is concisely expressed by the condition $\Delta\Omega.\tau_{max} << 1$, where τ_{max} is the maximum travel time across the array.

The signal at the m^{th} sensor due to the j^{th} source can be described as

$$s_{mj}(t) = \check{s}_j(t).\exp[i\Omega(t + \tau_{mj})] \qquad (5)$$

where τ_{mj} is the time difference of arrival of the plane-wave between the m^{th} sensor and the origin. To derive an expression for τ_{mj} we recognise that the path difference between the m^{th} sensor and the origin is given by:

$$\Delta_{mj} = \boldsymbol{p}_m.\boldsymbol{r}_j/r_j = (x_m.\cos\phi_j.\cos\varphi_j + y_m.\sin\phi_j.\cos\varphi_j + z_m.\sin\varphi_j) \qquad (6)$$

Therefore, the time difference of arrival between the m'th sensor and the origin is

$$\tau_{mj} = \Delta_{mj}/c = (x_m.\cos\phi_j.\cos\varphi_j + y_m.\sin\phi_j.\cos\varphi_j + z_m.\sin\varphi_j)/c \qquad (7)$$

Using the above fact and the Eqn. (4), Eqn. (5) can be written as

$$s_{mj}(t) = \check{s}_{mj}(t)\ exp(i\Omega t) \qquad (8)$$

where

$$\check{s}_{mj}(t) = \check{s}_j(t)\ exp(i\Omega\Delta_{mj}/c) \qquad (9)$$

The signal at m^{th} sensor due to all sources is a sum of individual contributions in view of the linearity of wave equation. So the total signal at m^{th} sensor given by:

$$\check{s}_m(t) = \Sigma_j\, \check{s}_{mj}(t) \qquad (10)$$

Eqn. (10) may be recast in the vector-matrix notation as

$$\check{\boldsymbol{s}}_m^{\Omega}(t) = \boldsymbol{A}^{\Omega}.\check{\boldsymbol{s}}_j^{\Omega}(t) \qquad (11)$$

where $\check{\boldsymbol{s}}_m^{\Omega}(t) = [\check{s}_1(t) \ldots \check{s}_M(t)]^T \in \boldsymbol{C}^{Mx1}$,

$\mathbf{A}^{\Omega} \in \boldsymbol{C}^{MxJ}$ whose $(m,j)^{th}$ element is given by

$[\mathbf{A}]_{mj} = \exp(i\Omega\Delta_{mj}/c)$, and

$\check{\boldsymbol{s}}_j^{\Omega}(t) = [\check{\boldsymbol{s}}_1(t) \ldots \check{s}_J(t)] \in \boldsymbol{C}^{Jx1}$

Note that $\check{\boldsymbol{s}}_m^{\Omega}(t)$ is a narrow band low-pass random signal which constitutes the envelope of the complex signal $\boldsymbol{s}_m^{\Omega}(t)$ received at the array, i.e., $\boldsymbol{s}_m^{\Omega}(t) = \exp(i\Omega t).\check{s}_m^{\Omega}(t)$.

The matrix $\boldsymbol{A}^{\Omega}$ can be viewed as a system transfer matrix representing a multiple input multiple output (MIMO) system with J complex inputs and M complex outputs [10]. The input vector is $\check{s}_j^{\Omega}(t) \in C^{Jx1}$ (vector of source envelopes at time snapshot (t) and the output vector is $s_m^{\Omega}(t) \in C^{Mx1}$ (vector of received narrow band sensor signal envelopes). Thus, in effect, the plane-wave model has made it possible to view the field as a MIMO system represented by the system transfer matrix $\boldsymbol{A}^{\Omega}$. The j^{th} column of the system matrix $\boldsymbol{A}^{\Omega}$, $\boldsymbol{A}_j = [\exp(i\Omega\Delta_{1j}/c) \ldots \exp(i\Omega\Delta_{Mj}/c)]^T \in \boldsymbol{C}^{Mx1}$ is the transfer vector between the j^{th} source and the receiver array at frequency Ω for the plane-wave field. Figure 3 shows the field distribution in range-depth plane due to a point source located at $r = 0, z = 500$ m in a 2 km deep ocean for plane-wave scenario. The signal transmitted from the depth of 500 m travels outward feeling no boundaries.

In the real ocean, free-field propagation approximation is not valid; the waves interact with the boundaries causing multiple interferences. Figure 4 simulates the sound propagation, due to rigid boundary at the top and bottom of the oceanic waveguide to show the presence of strong interference pattern. Ocean acts as a waveguide characterised by multi-modal acoustic propagation due to its top-bottom limited boundary conditions. A new set of models are required to describe the propagation of an acoustic wave in the ocean with proper boundary condition. This model should also be capable of considering the effect of variation in the sound speed.

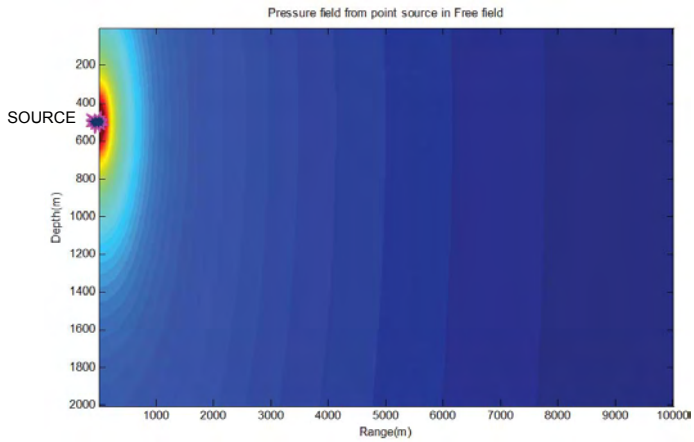

Figure 3. Free-field propagation: Spherical waves approximates a plane-wave in the far-field.

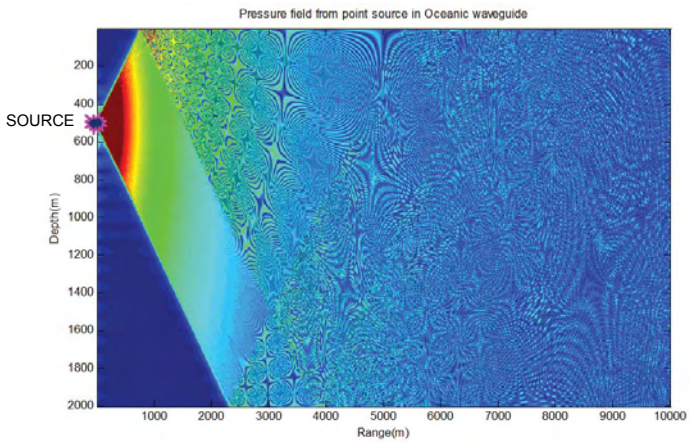

Figure 4. Waveguide propagation: Up-going and down-going waves interfere to produce the net field.

2.2 Oceanic Waveguide Propagation Model

A range-independent, horizontally stratified water layer of constant depth h meter (Fig. 5) overlying a horizontally stratified bottom [11] was considered. There are J narrowband sources of centre frequency Ω located at cylindrical range $r_{xy,j}$, depth z_j, and azimuth ϕ_j. There are M hydrophones located at range r_m, depth z_m, and azimuth ϕ_m. The sound speed variation along depth in the water layer ($z < h$) is $c(z)$ and $c_b(z)$ is the sound speed variation in the bottom layer ($z > h$). As stated above, the signal at m^{th} sensor due to j^{th} source is given by

$$s_{mj}(t) = p_{mj}\, \check{s}_j(t) \exp(i\Omega t) \quad (12)$$

where, p_{mj} is the pressure field at the m^{th} sensor due to j^{th} source in the ocean waveguide, $\check{s}_j(t)$ is the slowly varying zero-mean narrow band random process representing the envelope of the source signal. The pressure field p_{mj} is computed using the normal mode theory of wave propagation in an oceanic wave guide [12]. The normal mode solution to linear acoustic

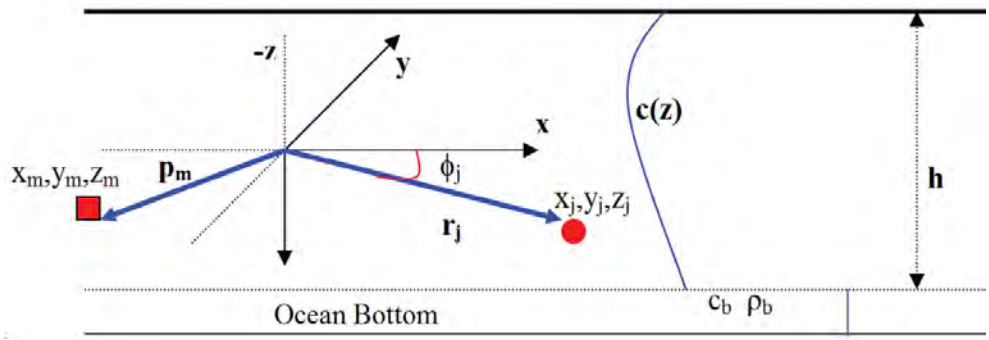

Figure 5. Source-receiver geometry in ocean wave-guide.

wave equation, in a horizontally stratified fluid medium, due to a point source located at depth z_j and at cylindrical range r_{mj} relative to the m^{th} sensor is given by

$$p_{mj} = \frac{i\pi}{\rho(z_j)} \sum_{n=1}^{\infty} \psi_n(z_j)\psi_n(z_m)H_0(k_n r) \tag{13}$$

where, $\rho(z_j)$ is the water density at depth z_j, $\psi_n(z)$ is the eigen-function corresponding to the n^{th} mode, k_n is the corresponding eigen value and $H_o(k_n r)$ is the bessel function of order 3 (also called the Hankel function). $P_n(z,r) = \psi_n(z)*H_o(k_n r)$, n = 1:inf are called the 'normal modes'. In practice one must limit the number of terms in Eqn. (13), for the pressure field computation, to some N_{max}. For the computation of the pressure field at far ranges N_{max} can be limited to the number of propagating modes (i.e., those which are total internally reflected from bottom) since the higher order modes decay rapidly due to bottom attenuation.

The mode functions and the mode values are computed using the popular KRAKEN program[12]. Given the sound speed profile (SSP), KRAKEN computes the mode-functions and the mode values associated with the range-invariant ocean. Then, according to the normal mode solution, the resulting pressure signal amplitude can be expressed as a weighted sum of several mode functions (Eqn. 13). Thus once the mode functions and the mode values have been computed for a particular medium, it is a simple task to compute the field at any point due to any point source in that medium. Eqn. (12) may be recast in the vector-matrix notation as

$$\check{\boldsymbol{s}}_m^{\Omega}(t) = \boldsymbol{A}^{\Omega}.\check{\boldsymbol{s}}_j^{\Omega}(t) \tag{14}$$

where $\check{\boldsymbol{s}}_m^{\Omega}(t) = [s_1(t) \ldots s_M(t)]^T \in \boldsymbol{C}^{Mx1}$, $\boldsymbol{A}^{\Omega} \in \boldsymbol{C}^{MxJ}$ whose $(m,j)^{th}$ element is given by $[\boldsymbol{A}]_{mj} = p_{mj}$, and

$$\check{\boldsymbol{s}}_j^{\Omega}(t) = [\check{s}_1(t) \ldots \check{s}_J(t)] \in \boldsymbol{C}^{Jx1}$$

Similar to the plane-wave case, the matrix $\boldsymbol{A}^{\Omega}$ can be viewed as a system transfer matrix representing a MIMO system with J complex inputs and M complex outputs. The inputs to this 'ocean-system' are monochromatic (single frequency) pressure signals emitted by J point-sources and the output is the pressure signal received at the array of sensors in the medium distinct from the source location.

3. BROADBAND SIGNAL SIMULATION

The broadband signal is synthesised by composing uniformly spaced narrow band signals over the band of interest. The bandwidth of the narrow band signal is chosen to satisfy the narrow band condition for the array processing mentioned in Section 2.1. This amounts to choosing the time-window of length T seconds such that the narrow band cell width $2\pi/T$ meets the required condition. Within a window, the envelope amplitude of the j^{th} source $\check{s}_j^{\Omega}(t)$ is held constant and, for every next window, $\check{s}_j^{\Omega}(t)$ is drawn independently from a zero-mean Gaussian distribution $\mathcal{N}(0,\sigma_j^2)$. This will in effect generate a narrow band signal of centre frequency Ω and bandwidth $2\pi/T$. To synthesise the discrete (or sampled) broadband signal one generates narrow band components at centre frequencies $\Omega_k = 2\pi k/T$, $k = 0,1,...,K$, where $K = FsT$, Fs being the sampling frequency meeting the Nyquist criterion. A sequence of complex numbers $\check{s}_j^k$ with $\mathrm{Re}\{\check{s}_j^k\} \sim \mathcal{N}(0,\sigma_j^2/2)$ and $\mathrm{Im}\{\check{s}_j^k\} \sim \mathcal{N}(0,\sigma_j^2/2)$ are drawn independently for each k =1,2,...,K once in every interval $NT \le t < (N+1)T$, N being the time block indexing integer. One can understand $\check{s}_j^k$ as the complex amplitude of the signal at frequency Ω_k held constant during the interval $NT \le t < (N+1)T$. Using Eqn. (11) or Eqn. (14) one may obtain the vector of received signal envelopes at the array of sensors, $\check{\boldsymbol{s}}_m^{\Omega}(t) = [\check{s}_1(t) \ldots \check{s}_M(t)]^T \in \boldsymbol{C}^{Mx1}$. Now by performing a K-point IFFT of the sequence $\{\check{s}_m^k: k = 1,2...K\}$, for each m at the N^{th} block index, we obtain the K-point broadband signal samples $\{s_m(n): n = NK, NK+1...NK+K-1\}$ for m = 1,2..., M during the N^{th} block period. By doing this for N = 0,1,2,... one can obtain the desired discrete broadband sequence $\{s_m(n): n = 0,1,2,...\}$ at each sensor, i.e. for m = 1,2..., M. This leads to a sequence of vectors $\{\boldsymbol{s}_m(n): n = 0,1,2,...\}$ that constitute signal portion of the observed/measured vector at the M-element array.

4. IMPLEMENTATION OF CONTINUOUS BROADBAND SIGNAL SIMULATION

Functions in Fig. 6 are implemented in MATLAB using standard functions. Sensor signals are generated block-wise whose period is the inverse of the frequency resolution of each narrow band cell. If Fs is the sampling frequency and K is the number of narrow band frequency cells, K/Fs is the simulation block time. The narrow band complex signal $S_j(k)$

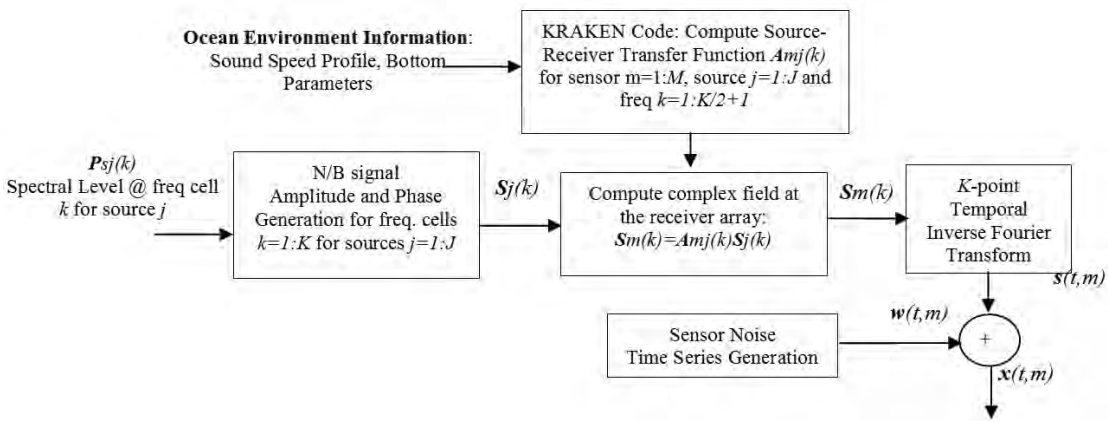

Figure 6. Functional block diagram for continuous broadband signal simulation.

at each frequency cell k and for each source j is drawn from a circular complex Gaussian distribution of mean zero and variance $P_{sj}(k)$, where $P_{sj}(k)$ is the power spectral density of source j at frequency k. The specification of $P_{sj}(k)$ allows to include narrow band tonal and modulation components if desired. The received complex field $Sm(k)$ at sensor m due to source j is then computed as $A_{mj}(k)S_j(k)$ for each frequency cell k. Computation of the medium-related transfer-function $A_{mj}(k)$ is based on whether the model is plane-wave or ocean acoustic modes, as explained in Section 2. The broadband signal $s_m(t)$ out of sensor m is then obtained through a K-point inverse Fourier transform of the sequence $\{S_m(k)\colon k=1\colon K\}$. The measured signal at sensor m is obtained by adding $s_m(t)$ with the noise time series $w_m(t)$.

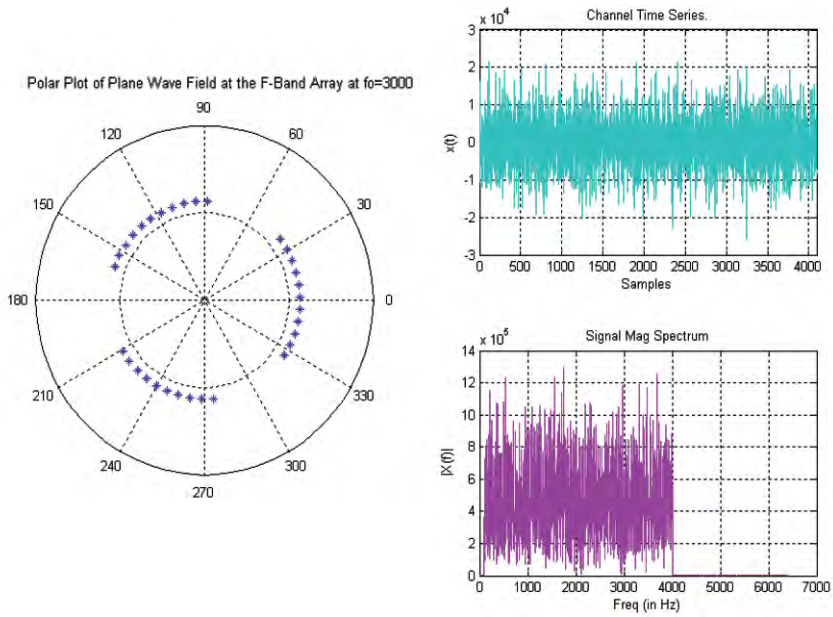

Figure 7. Polar plot of the plane-wave pressure field at the array.

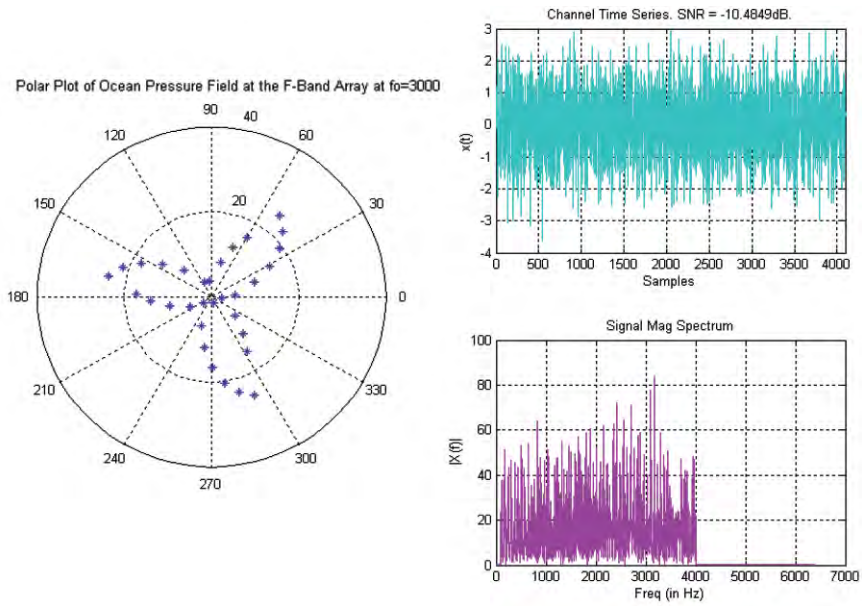

Figure 8. Polar plot of the ocean pressure field at the array.

4.1 Linear Array Signal Simulation

Towed sonar employs a linear hydrophone array towed behind a mother ship for sensing the acoustic field. The authors consider an array of 32 sensors uniformly spaced at an inter-element spacing of 17 cm. The inter-element distance of 17 cm, implies an upper cutoff operating frequency of 1500/(2*0.17) = 4.4 kHz for a plane-wave beam-former to avoid spatial aliasing. In the present study, the signals were simulated in 0.1-4 kHz operating band. Figure 7 depicts the polar plot of the pressure field for frequency f_o=3 kHz at sensors when exposed to a plane-wave from a target located along the end-fire axis of the array.

The inter-element phase delay for this frequency and for the target at 0 degree (wrt the axis of the array) works out to be $\Delta\phi = 2\pi f_o d/c = 2.13$ radian = 122.4 degrees, where d = 0.17 m and c = 1500 m/s. Therefore a plane-wave beam-former shall report the target at a conic angle of $\theta = \cos^{-1}(c\Delta\phi/2\pi f_o d) = 0$ degree as expected. Figure (8) shows the polar plot of the pressure field for frequency f_o =3 kHz at sensors when operated in an oceanic waveguide (assumed to be a Pekeris channel having water depth of 1 km, bottom speed 1700 m/s, and density ration of 2.0). In this case, a plane-wave beam-former reports a target at end-fire (at 5 km range and a depth of 30 m) to be at an angle of 24.48 degree (instead of 0 degree). This bias can be attributed to the vertical angle of arrival associated with each mode at frequency f_o. The shift in the vertical angle leads to bias in the angle estimated by the plane-wave beam-former which is significant for end-fire targets as shown in Fig. 9. For broadside targets, the wave from the target will continue to arrive through the ambiguous circular disk (response of 90 degree beam) about the array, although along a plane different from the azimuth plane, as shown in Fig. 10. In the case of left/right (L/R) resolving array employing triplet hydrophones (in lieu of mono-hydrophones), this vertical shift causes the null placed on the azimuth plane (at the opposite of main response axis of a beam) to be ineffective, thus impairing the discrimination performance.

The spectrum of the source signal (as received at 5 km) can be seen to be drastically modified by the channel under consideration (Fig. 11). Simulation from the plane-wave field shows little or almost no change in the received beam spectrum, even at a distance of 5km when the target is along the broadside. However, the oceanic waveguide modified the source signal broadband spectrum with null like and resonance like behaviours at certain frequencies. Hence passive signals spectrum received from target will be considerably

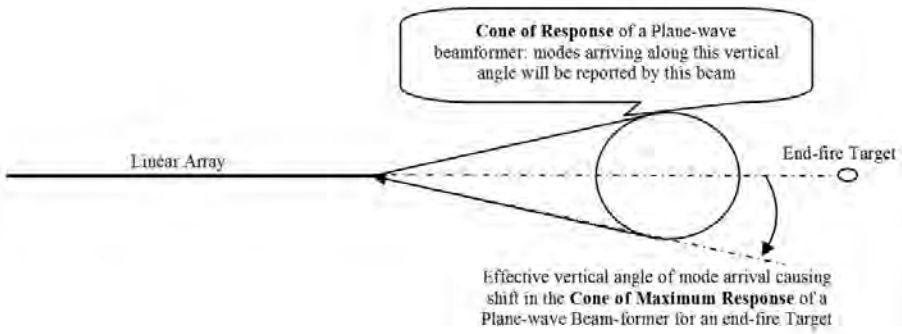

Figure 9. Shifting of the cone of maximum response for a target on end-fire of a linear array in oceanic waveguide.

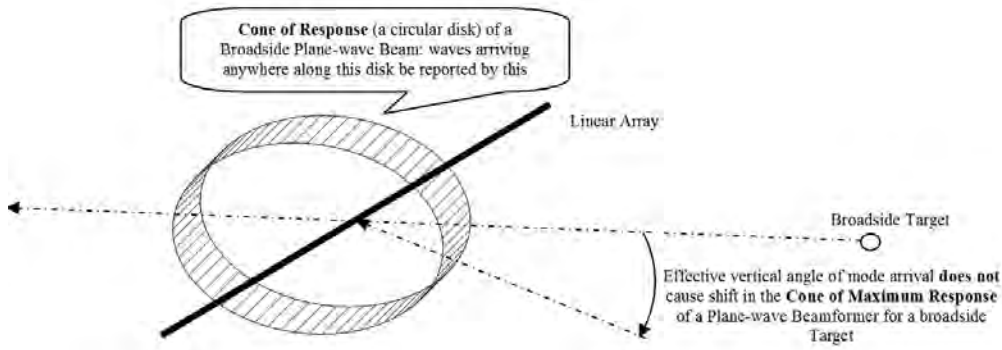

Figure 10. Target on broadside of a linear array in oceanic waveguide.

modified due to channel effect, making classification based on spectrum a difficult task. The channel effects have to be deconvolved from the received signal, to recover an approximation of the target signal in the absence of the channel. The subsequent classifier can be based on free-field scattering data. A variation of 8-10 dB in the lower frequency and 2-3 dB in the mid-frequency near 1000 Hz an 1700 Hz is observed from the graph. The pattern is subjected to change with the prevailing environmental condition.

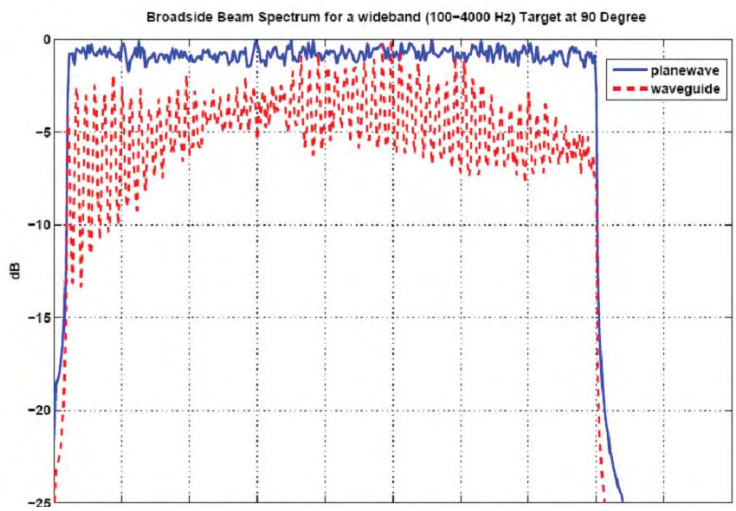

Figure 11. Average spectrum of the received signal at the array from a 100 Hz-4000 Hz wideband source located at 5 km from plane-wave and field due to oceanic waveguide.

As part of this work the software for sonar signal simulation in shallow ocean (S^4O,esQuado) in MATLAB® was developed, where-in it is convenient to run simulation for an arbitrary configuration (sonar, medium and source configuration). esQuado is capable of simulating continuous as well as pulsed broadband signal propagation in a shallow ocean. esQuado is based on the normal mode theory of acoustics. It invokes the compiled version of the popular KRAKEN program in MATLAB environment to compute the normal modes and its associated modal wavenumber. The mode functions and mode values need to be computed only once for a given site (where the experiment/trial is conducted) and is independent of the source-receiver geometry. Therefore, for a given environment, the signal simulation can be efficiently performed for arbitrary source-receiver geometry. Further this enables rapid assessment of transmit array deployment coordinates to maximise the contact illumination in the scan-mode of active sonar operation. esQuado provides a test input for studying the efficacy and robustness of several signal processing algorithms against effects such as multi-path and dispersive propagation, spectral modification due to the waveguide, etc.

5. SUMMARY AND CONCLUSIONS

The paper presents, theory of broadband sonar signal simulation in an oceanic waveguide presented along with some results and observation for the specific case of towed sonar. Specifically, it was shown that under typical

operating conditions of this sonar, multi-path and dispersion effects cannot be ignored as these lead to consideration deterioration in the performance of signal processing algorithms. Left/right discrimination performance is affected by the vertical angle of arrival of various modes in a waveguide. The shift in the vertical angle leads to bias in the angle estimated by the plane-wave beam-former which is significant for end-fire targets. Unlike the plane-wave propagation, propagation in an ocean waveguide results in considerable modification of the source signal broadband spectrum with null like and resonance like behaviours at certain frequencies depending on the environmental parameters. Hence, passive signals spectrum received from target will be considerably modified due to channel effect, making classification based on spectrum a difficult task. To assess and explain the effect of such phenomenon on system performance, a model has been developed to simulated broadband signals according to the wave equation for a top-bottom limited oceanic waveguide.

ACKNOWLEDGEMENTS

The authors are indebted to Dr MP Ajaikumar, DH(OA) and Shri PV Jose, PD (NAGAN) for bringing them together and constantly motivating them to pursue this work driven by the critical observations made during the sonar trials. The authors would also like to thank Director Sri S. Anantha Narayanan, Distinguished Scientist, NPOL for his permission and encouragement to present this work.

REFERENCES

1. Lakshmipathi & Anand, G.V. Subspace intersection method of bearing estimation in shallow water. *Signal Processing*, 2004, **84**, 1367-384.
2. Chouhan, Harish M. & Anand, G.V. Normal mode wave-number estimation using a towed array. *J. Acoust. Soc. Am*., 1993, **93**(4), 1807-181.
3. Sha, L. & Nolte, L. Bayesian sonar detection performance prediction in the presence of interference in uncertain environments. *J. Acoust. Soc. Am.*, 2005, **117**(4), 1954-964.
4. Sha, L. & Nolte, L. Effects of environmental uncertainties on sonar detection performance prediction. *J. Acoust. Soc. Am.,* 2005, **117**(4), 1942-953.
5. Goldhahn, R.; Hickman, G. & Krolikc, J. Waveguide invariant broadband target detection and reverberation estimation. *J. Acoust. Soc. Am*, 2008, **124**, 2841-851.
6. Tao, H. & Krolic, J. Waveguide invariant focusing for broadband beamforming in an oceanic waveguide. *J. Acoust. Soc. Am.*, 2008, **123**, 1338-346.
7. Hongwei, Liu; Paul, Runkle; Lawrence Carin; Timothy, Yoder; Thomas, Giddings; Luise, Couchman & Joseph, Bucaro. Classification of distant targets situated near channel bottoms. *J. Acoust. Soc. Am.*, 2004, **115**(3), 1185-197.
8. Angie, Sarkissian. Extraction of a target scattering response from measurements made over long ranges in shallows water. *J. Acoust. Soc. Am.,* 1997, **102**, 1997, 825-32.
9. Brekhowskikh & Lysanov, Yu P. Fundamentals of ocean acoustics. AIP Series, 2003.
10. Van Trees, H.L. Optimum array processing. detection, estimation, and modulation theory. Wiley Interscience, New York, 2002.
11. Frisk, G. Ocean and seabed acoustics: A theory of wave propagation. PTR Prentice-Hall, New York, 1994.
12. Porter, M.B. The KRAKEN normal mode program. SACLANT Undersea Research Centre, La Spezia, Italy, 1991. Report No. SM-245.
13. Jensen, Finn B.; Kuperman, William A.; Porter, Michael B. & Schmidt. Henrick Computational ocean acoustics. Springer-Verlag, 2000.

Contributors

Mr Baiju M. Nair completed his MSc (Physics) from Loyola College, Chennai, in 2001. He has worked in the field of electromagnetic wave propagation in microwaves devices and vacuum systems at MTRDC, Bengaluru. Presently he is working as Scientist at Naval Physical and Oceanographic Laboratory (NPOL), Kochi. His main areas of research include underwater sound propagation, underwater acoustic scattering from object and boundaries, environmentally adaptive algorithms, modelling, and acoustic data analysis.

Mr K.P. Arunkumar obtained his BTech. (Elect. & Electro. Engg.) from Government Engineering College, Thrissur, in 1998 and ME in Signal Processing from Indian Institute of Science, Bengaluru, in 2007. Currently, he is scientist at NPOL working in Sonar Signal Processing, since April 2000. His research interests include array signal processing, image and multidimensional signal processing, detection and estimation theory, time frequency analysis, and adaptive signal processing.

Mrs Sudha B. Menon received BTech (Elect. & Electro. Engg.) from Government Engineering College, Thrissur, in 1992 and MTech (Comp. & Info. Sc) from Cochin University of Science and Technology, Cochin, in 1994. She is currently working as a scientist at NPOL in the area of sonar signal processing. Her research interests include array signal processing, adaptive algorithms, and underwater acoustics.